scientific reports

Check for updates

OPEN

FBXO2 promotes the progression of papillary thyroid carcinoma through the p53 pathway

Wenke Guo[1], Yaoqiang Ren[2] & Xinguang Qiu[1]✉

Emerging evidence have demonstrated that F-box only protein 2 (FBXO2) is intimately associated with malignant tumor development and occurrence. However, neither the functions nor the molecular mechanisms underlying FBXO2 have been determined in the papillary thyroid carcinoma (PTC). The quantitative real-time PCR (qRT-PCR), western blotting and immunohistochemistry were carried out to detect the FBXO2 expression in PTC tissues. CCK-8 assay, EdU assay and flow cytometry were used to assess cell proliferation, cell cycle and apoptosis. The trans-well assay was conducted to determine the cell invasiveness. The effect of FBXO2 on PTC cell proliferation in vivo was observed through a subcutaneous tumor formation experiment in nude mice. Immunoprecipitation were conducted to detect the interaction between FBXO2 and p53. The ubiquitination assays were conducted to assess the regulation of p53 ubiquitination by FBXO2. FBXO2 was overexpressed in both PTC tissues and cell lines. FBXO2 expression positively correlated with PTC tumor size, lymphatic metastasis, and extramembranous invasion. Furthermore, silencing FBXO2 inhibited PTC cell proliferation and promoted apoptosis. The overexpression of FBXO2 significantly promotes PTC cell proliferation. Mechanistic studies revealed that FBXO2 could directly bind to p53 and promote its ubiquitination degradation. Knockdown of p53 partially reversed the progression arrest induced by FBXO2 Knockdown in PTC cells. FBXO2 knockdown inhibited PTC cell proliferation and promoted apoptosis by targeting p53 for ubiquitination and degradation. This process represents a research foundation for its diagnostic and therapeutic applications.

Keywords FBXO2, Papillary thyroid carcinoma, Proliferation, Apoptosis, p53, Ubiquitination

Thyroid carcinoma (THCA) is one of the most common types of cancer in the endocrine system worldwide[1]. Papillary thyroid carcinoma (PTC) accounts for 80–90% of all cases and shows a steadily increasing incidence and morbidity rate[2]. Typically, PTC patients present with hard, single, or multiple thyroid masses. A positive prognosis can be achieved with thyroidectomy and radioactive iodine treatment in the early stages[3]. However, if metastasis is present, the recurrence rate increases significantly[4], highlighting the need for further exploration of the molecular mechanisms behind PTC to develop more effective treatments.

F-box only protein 2 (FBXO2), also known as FBG1 or Fbs1, is a cytoplasmic protein and ubiquitin ligase with high-mannose glycoprotein specificity[5]. FBXO2 plays a significant role in regulating normal and abnormal neuron functions as a ubiquitin-mediated degrader of several neuron glycoproteins[6]. In addition, it has been reported that FBXO2 targets insulin receptors for degradation by ubiquitin, thereby modulating insulin signaling[7]. Recently, emerging evidence demonstrated that FBXO2 was also strongly associated with the occurrence and development of malignant tumors, including gastric cancer and colorectal cancer[8,9]. However, whether FBXO2 plays a role in PTC remains completely unknown.

The tumor suppressor protein p53, known as the "guardian of the genome", has been extensively studied for nearly 40 years[10], coordinating cellular responses to genotoxic stress, and playing a regulatory role in a range of biological processes such as autophagy, apoptosis, cell cycle arrest, metabolism, and aging[11,12]. Despite being inactivated in 50% of human malignancies, only 10% of PTC have been found to have p53 mutations, and their role in thyroid cancer remains unclear[13].

In this study, we demonstrated that FBXO2 is overexpressed in both PTC tissues and cell lines, indicating its critical role in the pathogenesis of PTC. Moreover, FBXO2 knockdown suppressed the growth of THCA cell

[1]Department of Thyroid Surgery, The First Affiliated Hospital of Zhengzhou University, Zhengzhou, Henan, China. [2]Department of Urology, Fenyang Hospital of Shanxi Province, Lüliang, Shanxi, China. ✉email: fccqiuxg@zzu.edu.cn

lines and induced apoptosis by targeting p53 for ubiquitination and degradation, highlighting its potential as a novel therapeutic target for PTC.

Materials and methods

Patient tissue specimens and cell lines

We obtained 94 pairs of adjacent normal tissues and THCA tissues from The First Affiliated Hospital of Zhengzhou University after obtaining permission from the Institutional Review Board and obtaining informed consent from patients (2021-KY-0202-002). Clinicopathological characteristics of patients are listed in Supplementary Table 1. In addition, we also obtained THCA cell lines (HTh-7, B-CPAP, TPC-1, KTC-1 and CAL62) and normal human thyroid follicular epithelial cell (Nthy-ori3-1) from the Chinese Academy of Sciences (Shanghai, China). All cells were cultured in a humidified incubator at 37 °C with 5% CO_2 in DMEM medium (Gibco) supplemented with 10% fetal bovine serum (Gibco) and 1% penicillin-streptomycin (Gibco).

Cell transfection

Small interfering RNA (siRNA) against FBXO2 (siFBXO2) and p53 (sip53) were purchased from RiboBio (Guangzhou, China). siRNAs (50 nM) were transfected into TPC-1 and KTC-1 cells using Lipofectamine 2000 (Invitrogen) according to the manufacturer's instructions. The sequence of siRNAs targeting FBXO2 or p53 are shown in Supplementary Table 2. The pcDNA3.1-NC and pcDNA3.1-FBXO2 (overFBXO2) were purchased from GenePharma (Shanghai, China). The plasmids were transfected into cells by using Lipofectamine 2000 (Invitrogen) according to the manufacturer's instructions. The transfected cells were selected with Neomycin for 3–4 weeks.

RNA extraction and PCR assay

Total RNA was extracted using TRIzol kits (Invitrogen, Carlsbad, CA, USA) according to the manufacturer's instructions. Subsequently, quantitative real-time PCR (qRT-PCR) was performed using a StepOnePlus Real-Time PCR System (Applied Biosystems, Carlsbad, CA, USA) in accordance with a previous study[14]. The primers used in this experiment are listed in Supplementary Table 2, and they were obtained from Sangon Biotech (Shanghai, China). GAPDH was used as the internal control.

Western blot analysis

Cells were lysed with a cleavage buffer containing RIPA (Invitrogen), and their concentrations were determined by the BCA Protein Kit (Beyotime, China). The total proteins were separated by 12% or 10% SDS-PAGE and then transferred onto polyvinylidene difluoride membranes. After being blocked with 10% skim milk at room temperature for 1 h, the membranes were incubated with the primary antibody overnight at 4 °C. Subsequently, specific fluorescent-dye conjugated secondary antibodies were added to visualize the protein bands. The membranes were then incubated with the specific fluorescent-dye conjugated secondary antibodies (Li-Cor Biosciences) at room temperature for 1 h. Images were obtained and analyzed using the Odyssey® CLX Infrared Imaging System (Gene Company Limited, Shanghai, China) and ImageJ software. Antibodies against FBXO2 (Cat No. ab133717), p53 (Cat No. ab32389), p21 (Cat No. ab109199) Bax (Cat No. ab32503), Bcl-2 (Cat No. ab182858), Caspase-3 (Cat No. ab32351), Cleaved Caspase-3 (Cat No. ab182858) purchased from Abcam (Cambridge, UK) and β-actin (Cat No. 23660-1-AP) purchased from Proteintech Group (Wuhan, China).

Immunohistochemistry (IHC) analysis

We demonstrated the presence and location of FBXO2 in THCA tissue samples through IHC analysis with the corresponding anti-FBXO2 polyclonal antibody (Proteintech Group, Cat No. 14590-1-AP). An Olympus FSX100 microscope (Olympus, Japan) was used to capture and analyses images. 400-fold magnification was used for examining the IHC stained sections with Image-Pro Plus version 6.0 (Media Cybernetics, MD, USA).

Cell counting Kit-8 (CCK-8) assay

Cell viability was assessed using the CCK-8 assay. Cell proliferation activity was measured at 0, 24, 48, and 72 h after inoculating transfected cells (5,000 cells/100 μL/well) in 96-well plates. Briefly, the transfected cells were incubated for two hours with 10 μL of CCK-8 solution (Servicebio) added to each well at the indicated times. The optical density at 450 nm wavelength was determined using a spectrophotometer (Thermo Fisher Scientific, MA, USA).

5-Ethynyl-20-deoxyuridine assay (EdU) assay

The EdU assay was employed to evaluate cell proliferation viability using the EdU kit (Cell Light EdU DNA imaging Kit, RiboBio) as per the manufacturer's instructions. Briefly, transfected RCC cells were incubated for 2 h with EdU (100 mmol/L) in 96-well plates, followed by fixation with 4% formaldehyde for 30 min. Subsequently, the cells were incubated with Apollo staining solution for 30 min following permeabilization with 0.5% Triton-X. Finally, the fluorescence of the cells was detected using a fluorescence microscope (Olympus) and the images were analyzed. Cell proliferation viability was measured by the ratio of EdU-stained cells (red fluorescence) to Hoechst-stained cells (blue fluorescence).

Cell cycle assay

The cells were harvested and fixed in 75% ethanol for 30 min at room temperature, then stained with propidium iodide buffer (BD Pharmingen) for 30 min. Subsequently, flow cytometry (Becton Dickinson, NJ, USA) was used to analyze the cells in the samples and ModFit LT was employed to analyze the results.

Mouse xenograft assay

Ten male nude mice were procured from Shanghai Animal Laboratory Center (Shanghai, China) and allocated into two groups. TPC-1 cells were injected subcutaneously into the hip back of mice. A week later, the vivo-optimized antisense oligonucleotides (ASOs) (RiboBio, Guangzhou, China) and its normal control were locally injected into the tumor mass once every 3 days for 3 weeks (5 nmol ASOs or normal control RNA dissolved in 50 μL of sterile PBS). The volume of the tumor was measured on a weekly basis. After four weeks, the animals were sacrificed and the weight of the tumors was recorded. For the overexpression experiment, TPC-1 cells stably transfected with overFBXO2 plasmids or control plasmids were subcutaneously injected into the right flanks of the nude mice, respectively. Three weeks later, the animals were euthanized and the weight of the tumor was recorded. The volumes of tumors were measured as the length×width^2×0.5. This experiment was conducted with the approval of the Ethical Committee of the First Affiliated Hospital of Zhengzhou University (2021-KY-0202-002).

Cell apoptosis assay

At 72 h post-transfection, cells were collected and stained using the Annexin V-PI Apoptosis Detection Kit (BD Pharmingen) according to the manufacturer's instructions. Apoptosis rate was then assessed by flow cytometry (ACEA NovoCyte3130, ACEA Biosciences Inc., China).

Immunoprecipitation (IP) and GST-pulldown assay

Cells were collected and lysed to extract proteins with IP buffer according to the manufacturer's instructions (Servicebio). Binding total protein with target antibodies against p53 (Abcam, ab26) or FBXO2 (Proteintech Group, 14590-1-AP) overnight to form antigen antibody complexes, followed by incubation with Protein A and G Sepharose (Life Technologies) for 2 h at 4 °C. IgG antibody as control. Then, wash the beads three times with wash buffer to remove nonspecifically bound proteins. Finally, separated on 12% SDS-PAGE for immunoblot analysis. GST-pulldown assay was performed as described[15]. Briefly, HA-p53 protein was produced in 293T cells transfected with HA-p53 plasmids, then immunoprecipitated with anti-HA resin and eluted with HA peptide. The eluted HA-p53 was incubated with GST or GST-tagged FBXO2 in PB buffer at 30 °C for 2 h, followed by a 30-minute incubation with glutathione beads. The beads were washed, treated with SDS buffer, boiled, and subjected to SDS-PAGE for immunoblotting analysis.

In vivo ubiquitination assays

In brief, cells were treated with 10 μM MG132 for 8 h, followed by collecting for ubiquitination assays. The levels of p53 ubiquitination in cells were determined by immunoprecipitation with an anti-p53 antibody (Abcam, ab26) followed by western blotting analysis with an anti-HA antibody (Proteintech Group, 80992-1-RR).

Bioinformatics analysis

RNA-sequencing expression (level 3) profiles were retrieved from the TCGA dataset (https://portal.gdc.com) and GTEx (https://www.huaplusmd.com). Gene Set Enrichment Analysis (GSEA) was used to evaluate pathways enrichment in the gene set, based on a false discovery rate (FDR) < 0.25 and a nominal p-value < 0.05.

Statistical analysis

All statistical analyses were conducted using GraphPad Prism 7.0 (La Jolla, USA). Differences between groups were evaluated using Student's t-test or chi-square with mean ± standard error of the mean (SEM). One-way ANOVA was Used to compare the difference between three or more samples/groups of a single independent variable. A p-value < 0.05 was considered to indicate a significant difference.

Results

FBXO2 is overexpressed in PTC tissues and cell lines

In order to identify the expression level of FBXO2 in thyroid carcinoma tissues and normal tissues, we analyzed the TCGA and GTEx datasets. The results indicated that FBXO2 mRNA expression was significantly higher in THCA tumor tissues (Fig. 1a, b), and the level of FBXO2 increased with lymph node metastasis (Fig. 1c). However, the expression of FBXO2 is not correlated with TNM staging of PTC patients (Supplementary Fig. 1a). Additionally, we compared PTC tissues with their matched normal adjacent tissues from our hospital through qRT-PCR or immunohistochemistry assays. The results showed that FBXO2 mRNA and protein expression levels were significantly higher in PTC tissues compared to their corresponding normal thyroid tissues (Fig. 1d, e). Furthermore, a positive correlation was observed between FBXO2 upregulation in PTC patients and clinical indicators, including PTC tumor size, lymphatic metastasis, and extramembranous invasion (Supplementary Table 1). In accordance with the findings from tissues, FBXO2 mRNA and protein were also detected at higher levels in THCA cell lines (HTh-7, B-CPAP, TPC-1, KTC-1 and CAL62) than in Nthy-ori3-1 cells (Fig. 1f–h), especially PTC cell lines TPC-1 and KTC-1. Therefore, we further explore the biological role and mechanism of FBXO2 in TPC-1 and KTC-1 cell lines. The images from IF analysis showed that FBXO2 was mainly localized in the cytoplasm of PTC cells (Fig. 1h). These results indicated that FBXO2 might promote PTC progression.

FBXO2 regulates PTC cell proliferation and apoptosis

Given that FBXO2 was found to be overexpressed in PTC tissues and cell lines in our study, we further explored whether inhibition of FBXO2 could affect PTC cell biological activity. To this end, three siRNAs targeting the coding region of FBXO2 (siFBXO2) were designed and their knockdown efficiency was evaluated using qRT-PCR and western blotting (Fig. 2a, b). Notably, the most efficient siFBXO2-1 and siFBXO2-2 were selected for further studies. CCK-8 cell viability and EdU assays revealed that the knockdown of FBXO2 significantly reduced

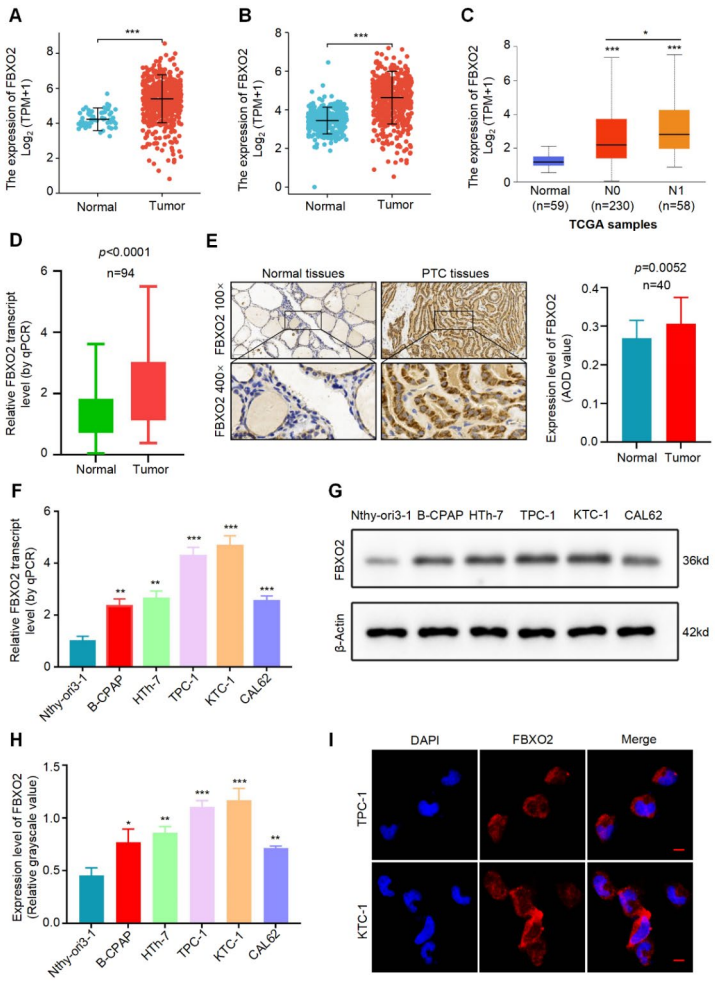

Fig. 1. FBXO2 is overexpressed in PTC tissues and cell lines. (**A**) The mRNA expression levels of FBXO2 in normal tissues ($n = 59$) and human THCA tissues ($n = 505$) from the TCGA database. (**B**) The mRNA expression levels of FBXO2 in normal tissues ($n = 338$) and human THCA tissues ($n = 512$) from the TCGA and GTEx database. (**C**) Expression of FBXO2 in THCA based on nodal metastasis status. Normal vs. N0 or N1; N0 vs. N1. (**D**) According to qRT-PCR results, PTC tissues expressed significantly more FBXO2 mRNA than adjacent healthy tissues. (**E**) Staining of samples with immunohistochemistry (IHC) revealed the levels of FBXO2 protein expression. The tumor sample shown here is stage T2N1aM0. (**F–H**) qRT-PCR (**F**) and western blotting analysis (**G**,**H**) were performed on Nthy-ori3-1 and THCA cell lines (HTh-7, B-CPAP, TPC-1, KTC-1 and CAL62) to determine the mRNA and protein levels of FBXO2. (**I**) Immunofluorescence (IF) showed that FBXO2 protein stained red was localized in cytoplasm of PTC cells. Nuclei were stained blue with DAPI (scale bar, 10 μm). Three independent replicates are used to calculate the mean ± SEM. $^{*}P < 0.05$, $^{**}P < 0.01$, $^{***}p < 0.001$ vs. Normal group (Student's t test).

the proliferation ability of PTC cells compared to the cells transfected with siNC (Fig. 2c, d). Moreover, cell cycle assays showed that FBXO2 knockdown increased the cellular proportions in the G0–G1 phase and decreased the cellular proportions in the S phase (Fig. 2e). Meanwhile, we found that silencing FBXO2 significantly reduced the cyclin D1 in TPC-1 and KTC-1 cells (Fig. 2f). Consistently, the results from xenograft tumors showed that knockdown of FBXO2 represses the proliferation of PTC cells in vivo (Fig. 2g). In addition, we observed that knockdown of FBXO2 promoted the apoptosis of TPC-1 and KTC-1 cells as revealed by apoptosis assay (Fig. 2h). However, no significant effect on the migration of TPC-1 and KTC-1 cells was observed from the trans-well migration assay (Supplementary Fig. 1b, c). Collectively, these results indicate that FBXO2 knockdown inhibits PTC cells proliferation and promotes PTC cells apoptosis, which suggests a pro-tumor role for FBXO2 in PTC progression.

To further investigate the effects of FBXO2 overexpression on the biological functions of PTC cells, we constructed an FBXO2 overexpression vector and validated its efficiency through qRT-PCR and western blotting assays (Supplementary Fig. 2a, b). Using EdU assays and animal subcutaneous tumor models, we found that FBXO2 overexpression significantly promotes the proliferation of PTC cells (Supplementary Fig. 2c, d). However,

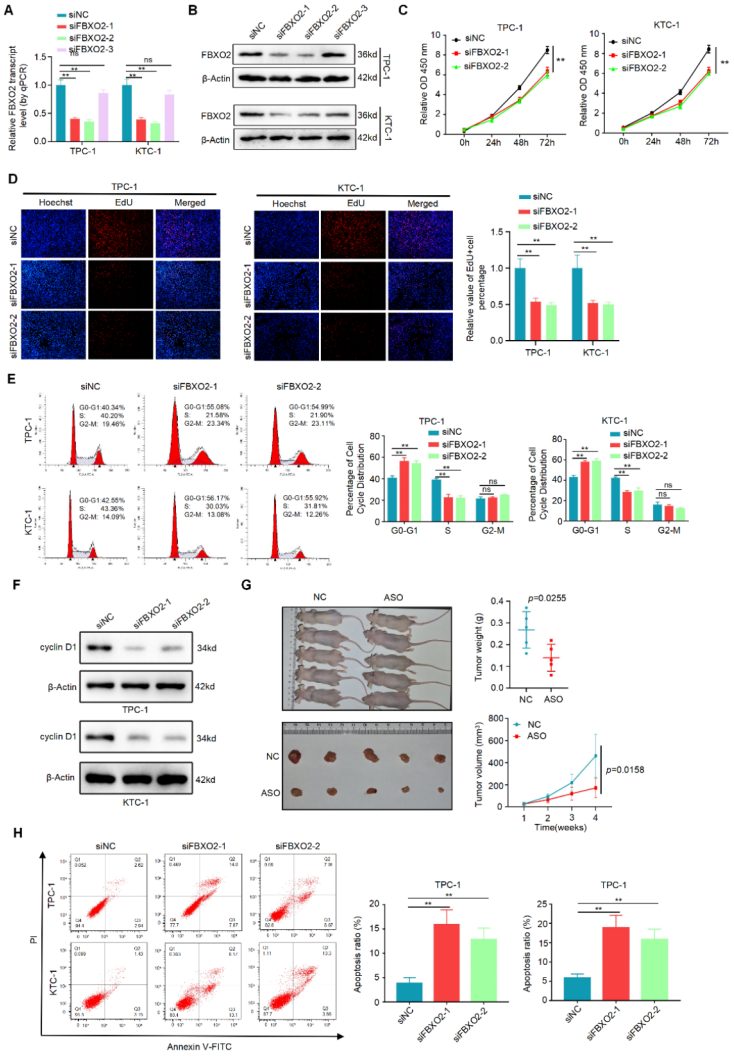

Fig. 2. Knockdown of FBXO2 inhibits PTC cells proliferation and promotes PTC cells apoptosis. (**A**,**B**) qRT-PCR (**A**) and western blot analysis (**B**) were performed on TPC-1 and KTC-1 cells. (**C**) Cell viability was then assessed using CCK-8 assays. (**D**) The proliferation of cells was detected by EdU assays. (**E**) Cell cycle arrest at G0/G1 phase was observed in TPC-1 and KTC-1 cells following knockdown of FBXO2 compared to their negative controls. (**F**) Western blotting were performed to determine the expression of cyclin D1 in TPC-1 and KTC-1 cells after knockdown of FBXO2. (**G**) Tumors collected from mice were exhibited, and the weights and volumes of xenograft tumors were measured and analyzed. (**H**) Cell apoptosis rates in siFBXO2 cells and corresponding control cells were detected by flow cytometry. Data are presented as mean ± SEM from three independent replicates. $^{**}P < 0.01$ (Student's t test).

due to the inherently low apoptosis rate of PTC cells, FBXO2 overexpression does not have a significant effect on apoptosis in these cells (Supplementary Fig. 2e).

FBXO2 targets p53 for ubiquitination and degradation

To further elucidate the underlying mechanism of FBXO2 in TPC-1 and KTC-1 cells, GSEA analysis was performed using the TCGA database. These results suggested that FBXO2 might participate in the regulation of p53 signaling pathway (Fig. 3a, b). To verify this, we tested the expression of p53 and its downstream molecules involved in the cell cycle and apoptosis. Western blot analysis revealed that knockdown of FBXO2 promoted the expression of p53 at the protein level, but not the mRNA level (Fig. 3c, d). In addition, the expression of downstream target genes of p53, such as p21, Bax, Bcl-2, caspase3 and cleaved caspase3, were found to be affected by FBXO2 knockdown (Fig. 3e). Furthermore, we found that knockdown of FBXO2 decreased ubiquitination of endogenous p53 in TPC-1 cells (Fig. 3f). Next, we performed an immunoprecipitation (IP) assay to verify the interaction between FBXO2 and p53. Our results showed that p53 was readily detectable in the immunoprecipitates of Flag-FBXO2 (Fig. 3g). The results from in vivo binding assays further confirms that the interaction between FBXO2 and p53 protein (Fig. 3h). In addition, GST-FBXO2 protein, but not GST protein alone, captured HA-p53 protein produced in the 293T cells (Fig. 3i). We conducted CHX treatment to inhibit

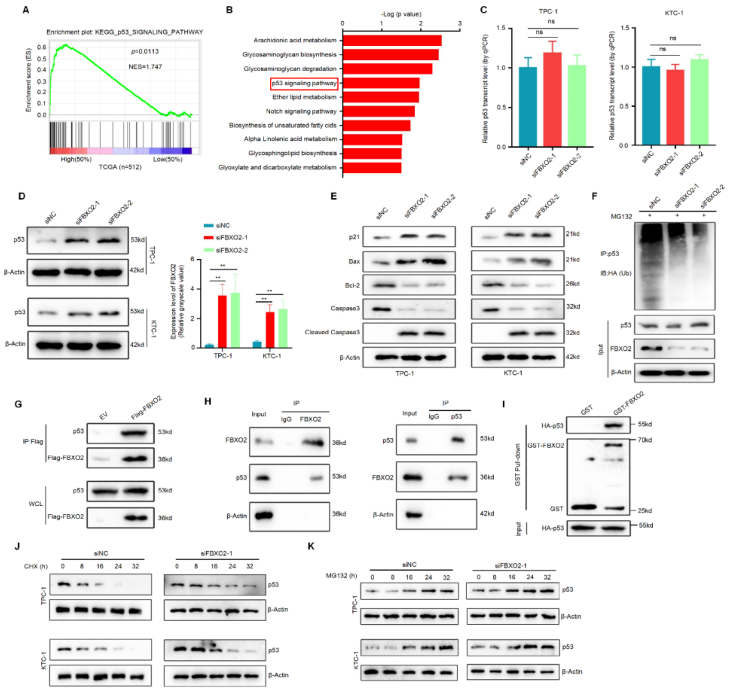

Fig. 3. FBXO2 targets p53 for ubiquitination and degradation. (**A**,**B**) Gene set enrichment analysis (GSEA) of FBXO2 mRNA and thyroid carcinoma signaling pathways was performed. FDR < 25% and $P < 0.05$ were considered significant. (**C**,**D**) qRT-PCR (**C**) and western blotting (**D**) were carried out to detect the expression of p53 in TPC-1 and KTC-1 cells. (**E**) Western blotting to detect the effect of siFBXO2 on the expression of downstream target genes of p53-related proteins. (**F**) Ectopic expression of FBXO2 promoted ubiquitination of p53 in TPC-1 cells analyzed by in vivo ubiquitination assays. Ub, ubiquitin. (**G**) 293T cells were transfected with either FLAG-Con or Flag-FBXO2 for 36 h. Four hours prior to harvesting, MG132 was added. The cells were then lysed, and immunoprecipitation was performed using Flag M2 beads. Proteins bound to the beads were eluted with Flag peptide and analyzed by immunoblotting with anti-FLAG and anti-p53 antibodies. (**H**) The cell lysates of TPC-1 cells were subjected to immunoprecipitation with IgG or anti-FBXO2 or anti-p53 antibody and then detected by immunoblotting with indicated antibodies. (**I**) 293T cells transfected with HA-p53 were lysed and then incubated with either GST alone or GST-FBXO2 immobilized on GST-Sepharose beads. The bound proteins were eluted using SDS loading buffer and detected by immunoblotting with the specified antibodies. (**J**) Cell lysates from siNC or siFBXO2 cells treated with 20 μg/ml cycloheximide (CHX) were subjected to western blotting with the p53 antibodies. (**K**) Cell lysates from siNC or siFBXO2 cells treated with 10 μM MG-132 were subjected to western blotting with the p53 antibodies. Three independent replicates are used to calculate the mean ± SEM (Student's t test).

protein synthesis and found that FBXO2 influenced p53 protein stability (Fig. 3j). The results from MG132 treatment experiments further demonstrate that FBXO2 regulates the stability of p53 through ubiquitination (Fig. 3k). Collectively, these results indicate that FBXO2 targets p53 for ubiquitination and degradation.

Knockdown of FBXO2 inhibits PTC cells proliferation and promotes PTC cells apoptosis through p53 pathway

We further investigated whether FBXO2 affected the biological activity of TPC-1 and KTC-1 cells by increasing the expression of p53 by using rescue experiments. Firstly, we designed three siRNAs targeting the coding region of p53 (sip53) and the knockdown effect of sip53-2 made it a strong candidate for further studies (Fig. 4a, b). Then, we performed cell cycle assay and the result showed that the cell cycle arrest induced by siFBXO2 was partially reversed through knocking down p53 (Fig. 4c). Consistently, siFBXO2-induced apoptosis increase was partially reversed by silencing of p53 (Fig. 4d). In summary, these results demonstrate that FBXO2 promoted PTC progression through p53 pathway.

Discussion

PTC is one of the most prevalent malignancies, characterized by a relatively low somatic mutation burden per tumor. However, PTC has been found to exhibit over 90% abnormal driver expression, which provides a selective growth advantage promoting cancer development[16]. The molecular pathogenesis of the majority of PTC involves dysregulation of BRAF, RAS, TERT, and p53 signaling pathways[16,17].

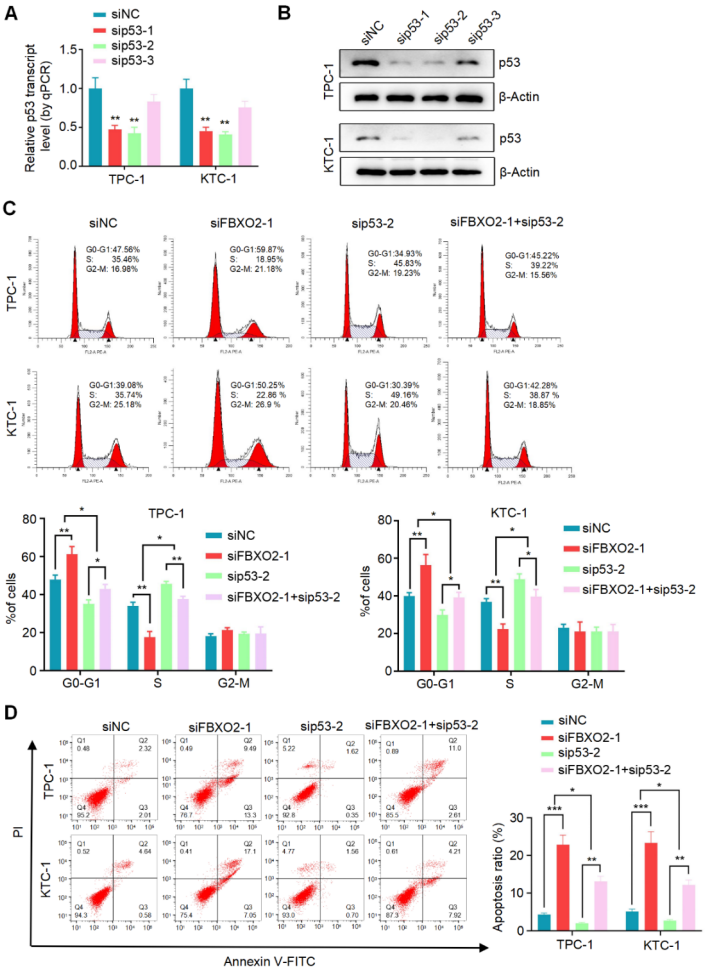

Fig. 4. Knockdown of FBXO2 inhibits PTC cells proliferation and promotes PTC cells apoptosis by increasing the expression of p53. (**A**,**B**) qRT-PCR (**A**) and western blotting (**B**) were performed to determine the efficiency of p53 knockdown in TPC-1 and KTC-1 cells. (**C**) In flow cytometry, cell cycle distributions were examined in siNC group, siFBXO2-1 group, sip53-2 group, and siFBXO2-1 + sip53-2 group. (**D**) Apoptotic cell death of TPC-1 and KTC-1 cells treated with siNC, siFBXO2-1, sip53-2, or siFBXO2-1 + sip53-2 for 48 h was analyzed by flow cytometry using Annexin V-FITC/PI double-staining kit. Three independent replicates are used to calculate the mean ± SEM. $^{*}P < 0.05$; $^{**}P < 0.01$ (Student's t test).

Polyubiquitination refers to the addition of an ubiquitin chain to a single lysine residue on a target protein, which typically results in the protein's degradation[18]. This process involves a three-step cascade of ubiquitin transfer that includes activation, conjugation, and ligation[19]. These steps are facilitated by three types of enzymes: ubiquitin-activating enzymes (E1s), ubiquitin-conjugating enzymes (E2s), and ubiquitin ligases (E3s)[20]. Among the E3 ligases, the largest subfamily in mammals is the Skp1-Cul1-F-box protein complex, which is composed of Skp1, Cul1, Rbx1, and a specific F-box protein (FBP)[21]. FBXO2, a member of the human F-box family, plays an essential role in the progression of cell cycle regulation[22]. FBXO2 was reported to promote endometrial carcinoma proliferation by regulating the autophagy signaling pathway and cell cycle through acting as an E3 ligase that degrades FBN1 in a ubiquitin-dependent manner[23]. Additionally, it has been reported that FBXO2 plays a crucial role in the proliferation of osteosarcoma cells by regulating the STAT3 signaling pathway[24]. In this study, we present the first evidence that FBXO2 is critically involved in the progression of PTC by regulating p53 expression through ubiquitination. This novel finding significantly advances the understanding of PTC molecular mechanisms.

P53 is a pivotal player in a multitude of cellular signaling pathways, being involved in cell cycle progression, cell differentiation, DNA repair, and apoptosis[25,26]. When abnormally expressed, p53 can lead to checkpoint defects, genomic instability, and the inhibition of apoptosis, thus promoting thyroid carcinogenesis[27–29]. Moreover, its stability is regulated by the ubiquitin-dependent degradation of proteins[30]. However, our discovery that FBXO2 directly influences p53 ubiquitination and degradation in PTC cells represents a major step forward in unraveling the molecular underpinnings of PTC.

Importantly, our study is the first to reveal that FBXO2 mRNA and protein levels are elevated in PTC tissues and cell lines, with a significant correlation to tumor size, lymph node metastasis and extracellular invasion in PTC patients. By demonstrating that FBXO2 knockdown suppresses PTC cell proliferation and promotes apoptosis through the targeting of p53 for ubiquitination and degradation, our research provides fresh insights into the molecular mechanisms driving PTC progression. This discovery not only enhances the understanding of PTC but also suggests potential therapeutic avenues targeting FBXO2-p53 interactions. In our future research, we will further explore the structural domains of FBXO2 that bind to p53 and investigate other biological functions of FBXO2 that may contribute to cancer progression.

In conclusion, our study identifies FBXO2 as a novel regulator of p53 in PTC, providing a new perspective on the molecular pathology of PTC and opening up potential new therapeutic strategies.

Data availability

All data generated or analysed during this study are included in this published article and its supplementary information files.

Received: 25 February 2024; Accepted: 17 September 2024
Published online: 29 September 2024

References

1. Miller, K. D. et al. Cancer treatment and survivorship statistics, 2022. *CA Cancer J. Clin.* **72** (5), 409–436 (2022).
2. Cui, L. et al. Clinical outcomes of multifocal papillary thyroid cancer: a systematic review and meta-analysis. *Laryngosc. Investig. Otolaryngol.* **7** (4), 1224–1234 (2022).
3. Zhang, L. et al. Molecular basis and targeted therapy in thyroid cancer: Progress and opportunities. *Biochim. Biophys. Acta Rev. Cancer* **1878** (4), 188928 (2023).
4. Ge, M. H. et al. Nomograms predicting disease-specific regional recurrence and distant recurrence of papillary thyroid carcinoma following partial or total thyroidectomy. *Med. (Baltim.)* **96** (30), e7575 (2017).
5. Zhang, H. J. & Tian, J. Epstein-Barr virus activates F-box protein FBXO2 to limit viral infectivity by targeting glycoprotein B for degradation. *PLoS Pathog.* **14** (7), e1007208 (2018).
6. Atkin, G. et al. Loss of F-box only protein 2 (Fbxo2) disrupts levels and localization of select NMDA receptor subunits, and promotes aberrant synaptic connectivity. *J. Neurosci.* **35** (15), 6165–6178 (2015).
7. Liu, B. et al. Aberrant expression of FBXO2 disrupts glucose homeostasis through ubiquitin-mediated degradation of insulin receptor in obese mice. *Diabetes* **66** (3), 689–698 (2017).
8. Sun, X. et al. FBXO2, a novel marker for metastasis in human gastric cancer. *Biochem. Biophys. Res. Commun.* **495** (3), 2158–2164 (2018).
9. Wei, X. et al. The prognostic significance of FBXO2 expression in colorectal cancer. *Int. J. Clin. Exp. Pathol.* **11** (10), 5054–5062 (2018).
10. Dolgin, E. The most popular genes in the human genome. *Nature* **551** (7681), 427–431 (2017).
11. Levine, A. J. p53, the cellular gatekeeper for growth and division. *Cell* **88** (3), 323–331 (1997).
12. Vousden, K. H. & Prives, C. Blinded by the light: the growing complexity of p53. *Cell* **137** (3), 413–431 (2009).
13. Malaguarnera, R. et al. p53 family proteins in thyroid cancer. *Endocr. Relat. Cancer* **14** (1), 43–60 (2007).
14. Gu, C. et al. Mettl14 inhibits bladder TIC self-renewal and bladder tumorigenesis through N(6)-methyladenosine of Notch1. *Mol. Cancer* **18** (1), e168 (2019).
15. Ji, J. et al. FBXO2 targets glycosylated SUN2 for ubiquitination and degradation to promote ovarian cancer development. *Cell. Death Dis.* **13** (5), 442 (2022).
16. Prete, A. et al. Update on fundamental mechanisms of thyroid cancer. *Front. Endocrinol. (Lausanne)* **11**, e102 (2020).
17. Feng, J. et al. A novel lncRNA n384546 promotes thyroid papillary cancer progression and metastasis by acting as a competing endogenous RNA of mir-145-5p to regulate AKT3. *Cell. Death Dis.* **10** (6), e433 (2019).
18. Hoeller, D. & Dikic, I. Targeting the ubiquitin system in cancer therapy. *Nature* **458** (7237), 438–444 (2009).
19. Vucic, D., Dixit, V. M. & Wertz, I. E. Ubiquitylation in apoptosis: a post-translational modification at the edge of life and death. *Nat. Rev. Mol. Cell. Biol.* **12** (7), 439–452 (2011).
20. Skaar, J. R., Pagan, J. K. & Pagano, M. SCF ubiquitin ligase-targeted therapies. *Nat. Rev. Drug Discov.* **13** (12), 889–903 (2014).
21. Zheng, N., Wang, Z. & Wei, W. Ubiquitination-mediated degradation of cell cycle related proteins by F-box proteins. *Int. J. Biochem. Cell. Biol.* **73**, 99–110 (2016).
22. Erhardt, J. A. et al. A novel F box protein, NFB42, is highly enriched in neurons and induces growth arrest. *J. Biol. Chem.* **273** (52), 35222–35227 (1998).
23. Che, X. et al. FBXO2 promotes proliferation of endometrial cancer by ubiquitin-mediated degradation of FBN1 in the regulation of the cell cycle and the autophagy pathway. *Front. Cell. Dev. Biol.* **8**, e843 (2020).
24. Zhao, X. & Guo, W. FBXO2 modulates STAT3 signaling to regulate proliferation and tumorigenicity of osteosarcoma cells. *Cancer Cell. Int.* **20**, e245 (2020).
25. Böhlig, L. & Rother, K. One function–multiple mechanisms: the manifold activities of p53 as a transcriptional repressor. *J. Biomed. Biotechnol.* **2011**, e464916 (2011).
26. Bellazzo, A. et al. Complexes formed by mutant p53 and their roles in breast cancer. *Breast Cancer (Dove Med. Press)* **10**, 101–112 (2018).
27. Meng, X. F., Zhao, L. Y. & Chu, X. F. LncRNA LINC00673 inhibits p53 expression by interacting with EZH2 and DNMT1 in papillary thyroid carcinoma. *Eur. Rev. Med. Pharmacol. Sci.* **23** (5), 2075–2083 (2019).
28. Yang, D. et al. Abnormality of pl6/p38MAPK/p53/Wipl pathway in papillary thyroid cancer. *Gland Surg.* **1** (1), 33–38 (2012).
29. Zou, M. et al. TSH overcomes Braf(V600E)-induced senescence to promote tumor progression via downregulation of p53 expression in papillary thyroid cancer. *Oncogene* **35** (15), 1909–1918 (2016).
30. Zhang, J. et al. ABRO1 suppresses tumourigenesis and regulates the DNA damage response by stabilizing p53. *Nat. Commun.* **5**, e5059 (2014).

Author contributions

W.G. was responsible for vitro experiments, conceived the idea, participated in the design of the study, performed xenograft tumor growth assay, participated in the analysis, and drafted the manuscript. Y.R. was responsible for vitro experiments and participated in the analysis. X.Q. conceived the idea, participated in the design of the study, and drafted the manuscript.

Funding
This work was supported by a grant from Thermal Ablation of Thyroid Nodules International Joint 726 Laboratory (Henan Province) (YUKEWAI [2016] NO.11).

Declarations

Competing interests
The authors declare no competing interests.

Ethical approval
The informed consent was signed by all participators. This study was proceeded after getting the approval of the Ethics Committees of the First Affiliated Hospital of Zhengzhou University. The study about animal experiment got authorization from the Experimental Animal Ethics Committee of Zhengzhou University (approval number: 2021-KY-0202-002) and performed in accordance with the guidelines of the National Animal Care and Ethics Institution. It was carried out in compliance with the ARRIVE guidelines.

Additional information
Supplementary Information The online version contains supplementary material available at https://doi.org/10.1038/s41598-024-73455-z.

Correspondence and requests for materials should be addressed to X.Q.

Reprints and permissions information is available at www.nature.com/reprints.

Publisher's note Springer Nature remains neutral with regard to jurisdictional claims in published maps and institutional affiliations.